ISSN 0006-2979, Biochemistry (Moscow), 2007, Vol. 72, No. 5, pp. 558-564. © Pleiades Publishing, Ltd., 2007.
Published in Russian in Biokhimiya, 2007, Vol. 72, No. 5, pp. 690-698.

Heterogeneity of Thylakoid Membranes Studied by EPR Spin Probe

S. M. Kochubey[1]*, A. I. Vovk[2], O. Yu. Bondarenko[1], V. V. Shevchenko[1], R. V. Bugas[2], A. K. Melnyk[2], and V. Yu. Tanchuk[2]

[1]Institute of Plant Physiology and Genetics, National Academy of Sciences of Ukraine, Vasilkovskaya str. 31/17, 03022 Kiev, Ukraine; fax: 380 (44) 258-8146; E-mail: skbiofis@naverex.kiev.ua
[2]Institute of Bioorganic Chemistry and Petrochemistry, National Academy of Sciences of Ukraine, Murmanska str. 1, 02660 Kiev, Ukraine; fax: 380 (44) 573-2552; E-mail: vovk@bpci.kiev.ua

Received November 14, 2006
Revision received January 23, 2007

Abstract—A lipophilic nitroxyl radical, 1-oxyl-2,2,6,6-tetramethylpiperidin-4-yl 1-adamantylacetate, has been applied to EPR spin probe study of chloroplasts and subchloroplast fragments of different types. The latter originate from grana and the grana core regions. The binding of the spin probe to the membranes was revealed by specific changes in a shape of the EPR spectra. A share of membrane-bound spin probe was different for chloroplasts and subchloroplast fragments, as well as its rotational correlation time and apparent enthalpy and entropy activation of nitroxide rotational motion. The binding of the spin probe induced a significant decrease in the amount of the oxidized P700 and changes in the kinetics of its light oxidation and dark recovery. This suggests that one of the sites of nitroxyl radical binding is the nearest surrounding of the pigment–protein complexes of Photosystem I (PSI). Distinctions in mobility of spin probe immobilized by chloroplasts and their fragments can be caused by the different environment of the PSI complexes located in various regions of thylakoid membranes.

DOI: 10.1134/S0006297907050136

Key words: chloroplasts, EPR, Photosystem I, spin probe, thylakoids

A specific feature in the thylakoid system of chloroplasts of higher plants is heterogeneity in their organization. Differences in structure and composition are inherent in intergranal and granal thylakoids. The latter contain differently organized core and margin regions [1-4]. Specific compartments are also so-called "end" membranes of grana. They are located at the boundary of grana and stroma, and all their area contacts the stroma [5, 6]. All these compartments differ in both structure and organization of the pigment–protein complexes, and also in character of the primary photoreactions which they realize [1-6]. It is also known that Photosystem I (PSI) complexes located in the grana margins of thylakoids (PSIα) differ in structure of protein components of light-harvesting antenna from the PSI complexes located in the intergranal thylakoids (PSIβ) [7]. Earlier we isolated such subchloroplast fragments as the grana and the grana core particles [8]. The fragments differ in chlorophyll/protein ratio, and also in fluorescence spectral characteristics [8]. Distinctions have been revealed in organization of PSI complexes located in these areas of thylakoids [7, 9, 10].

Stable nitroxyl radicals are widely used for studies of biological membranes, including photosynthetic ones [11, 12]. Various stearic acid spin probes bearing a free radical oxazolidine fragment at various positions along the hydrocarbon chain are applied to determined structural changes, dynamics, and functional activity of some sites in chloroplast structures [13]. The analysis of spectra of such radicals brings out in particular some conclusions in relation of possible sites of localization of a spin probe [13]. It is known that the water soluble 1-oxyl-2,2,6,6-tetramethylpiperidine (TEMPO) and 4-hydroxy-TEMPO is capable of binding with membranes [14, 15].

In this work we used 1-oxyl-2,2,6,6-tetramethylpiperidin-4-yl 1-adamantylacetate (ATEMPO) [16] as a spin probe for comparative characterization of chloro-

Abbreviations: ATEMPO) 1-oxyl-2,2,6,6-tetramethylpiperidin-4-yl 1-adamantylacetate; LHCII) light-harvesting complex of PSII; PSI (II)) Photosystem I (II); TEMPO) 1-oxyl-2,2,6,6-tetramethylpiperidine.

* To whom correspondence should be addressed.

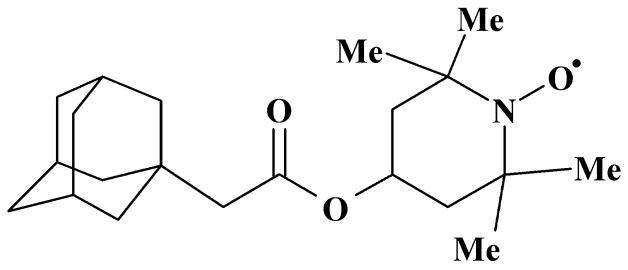

Fig. 1. Chemical structure of 1-oxyl-2,2,6,6-tetramethylpiperidin-4-yl 1-adamantylacetate (ATEMPO).

plasts and subchloroplast fragments. The chemical structure of this compound (Fig. 1) has a bulky carbocyclic fragment attached to the paramagnetic TEMPO residue. ATEMPO can be considered as a rather mobile and more hydrophobic spin probe in comparison with TEMPO. This feature of ATEMPO can cause its stronger immobilization in membranes. We investigated the interaction of this nitroxyl radical with chloroplasts and subchloroplast fragments such as grana system depleted of intergranal thylakoids and grana core particles.

MATERIALS AND METHODS

Pea chloroplasts with partially broken envelope were isolated as described earlier [9] in Tricine buffer (pH 7.5). Alcohol solution of ATEMPO was added to chloroplast suspension (1% of total suspension volume). The chlorophyll concentration was 1 mg/ml. The final concentration of ATEMPO was 5 mM. The mixture was incubated for 30 min in darkness at room temperature. Then it was centrifuged for sedimentation of the chloroplasts. The chloroplast pellet was resuspended and taken for measurements of EPR spectra. A part of the pellet was used for measurement of P700 kinetics. Some experiments were carried out with material washed free from residual probe. For this purpose, the chloroplast pellet was incubated with the probe as mentioned above, then it was repeatedly resuspended and centrifuged. Subchloroplast fragments of two types were isolated by solubilization of the chloroplasts with 0.3% digitonin and the subsequent differential centrifugation as described earlier [8, 17]. The fragments of the first type were suspension of grana from which intergranal thylakoids have been removed. They were contained in a pellet sedimented at 1000*g*. The fragments of the second type were the grana core particles that sedimented at 1300*g*. Further these fragments will be refered to as fragments 1 and 2, respectively. Alcohol solution of radical was added to suspensions of fragments 1 and 2, which contained chlorophyll at concentrations of 1 and 0.5 mg/ml, respectively. The final concentration of the added radical and the procedure of processing were the same as for chloroplasts. The washing of subchloroplast fragments to remove residual radical was carried out by the same protocol as for chloroplasts. In some experiments, EPR spectra of our stable radical were recorded for the supernatants above the pellets.

EPR spectra were registered on a Varian E-3 (USA) spectrometer using 0.8 mW microwave power, 100 kHz field modulation of 3.2 G, and Mn^{2+}/MgO as an internal standard. Samples were placed in 1.5 mm diameter glass capillaries, which were placed in a standard EPR tube. The temperature of the samples was changed in the range of 25-60°C using a V-4257 variable temperature controller and additionally checked by a thermocouple with accuracy of ±0.5°C. Preliminary experiments showed that the intensity of the EPR signal of the immobilized nitroxyl radical did not change under the measurement conditions. ATEMPO has been synthesized as described earlier [16]. EPR spectra were simulated using our own homemade software. Experimental data, represented by the first derivative of the field modulated EPR signal, were approximated by derivatives of asymmetric Gaussian bands. Starting peak positions were determined as maxima of the numerically integrated experimental curve. Parameters of the approximating Gaussians were fitted by a procedure based on the Breeder Genetic Algorithm [18]. The best results were obtained on the high-field lines, which were better resolved. Experimental spectra were also fitted by a linear combination of the narrow line spectra of radical in supernatants and wide line spectra obtained after washing of chloroplasts and subchloroplast fragments. Their linear combination gave the simulated spectra. The corresponding coefficients were determined by the least squares method.

For measurements of P700 oxidation kinetics, washed and unwashed chloroplasts and subchloroplast fragments of both types were used. Artificial donors or electron transport acceptors were not added to the suspension of chloroplasts or subchloroplast fragments. The testing of photosynthetic activity was carried out with measurements of P700 kinetics. The maximal intensity of P700 signal was measured at saturating actinic light. Measurements were carried out with an apparatus designed in our laboratory. P700 oxidation was detected by reduction of the optical density of a suspension at 700 nm. Suspension of chloroplasts or the fragments was placed in a 10 × 18 × 35-mm cuvette. Actinic illumination was directed in parallel to the side of the cuvette with the length of 18 mm. Several light-emitting diodes radiating at 440 nm were located along the height of two lateral sides of the cuvette at regular intervals. Such arrangement allowed us to reach a uniform light field inside the cuvette. Intensity of actinic light on the surface of the cuvette sides was 5 mW/cm^2, and it was saturating. Actinic light was modulated with frequency of 5 kHz to prevent influence of scattered actinic light and fluorescence onto the measured signal. Measuring light from an LED passed in a direction perpendicular to the actinic beam. It was fil-

tered with an interference filter with a transmission maximum at 700 nm and pass-band of 2 nm. The intensity of measuring light on the surface of the cuvette was 2 μW/cm^2. The optical density of suspension at 700 nm was monitored, and in our experiments it was in the range 0.5-0.7. The sensitivity of the apparatus was 0.001 optical density unit. The minimal step of sampling was 10 msec.

RESULTS

The EPR spectra of ATEMPO added to chloroplast pellets and subchloroplast fragments 1 and 2 are shown in Fig. 2, a-c. A change in the shape of the spectra occurs in comparison with the spectrum of the radical in supernatants showing the usual three-line pattern (Fig. 2d). The high-field lines in the EPR spectrum of nitroxide in chloroplasts and subchloroplast fragments are complex, consisting of two components with significantly different width (Fig. 2, a-c). After washing of chloroplasts and subchloroplast fragments, the narrow line components in the spectra of all our samples practically disappear (Fig. 3). This means that EPR spectra of ATEMPO consist of two components corresponding to various molecular tumbling of the spin probe. Analysis of the high-field lines can be used to display the components and estimate their intensities. The broader signal, obviously, corresponds to radical bound by membrane structures. Its high-field line is located inside the resulting spectrum (Fig. 2, a-c) because the isotropic hyperfine splitting constant is lower for the spin probe in the nonpolar than in polar microenvironment. The narrow line components of the EPR spectra can originate from the radical which is slightly bound by chloroplasts and their fragments, or from that radical fraction which is dissolved in residual amounts of aqueous buffer solution in the pellets. Disappearance of this component after washing of chloroplasts and the fragments (Fig. 3) confirms this supposition. This result indicates the presence of weakly immobilized or unbound radicals in unwashed material. It also indicates that the wide line component of the EPR spectrum really corresponds to strongly bound spin probe embedded into membrane.

The relative intensities of two components in EPR high-field lines appear different for chloroplasts and their fragments (Fig. 2, a-c). The fraction of strongly bound spin probe is the largest for chloroplasts. The partitioning of ATEMPO between the aqueous phase and the membranes (p) calculated as an intensity ratio of narrow and wide high-field line components shows the lowest value for chloroplasts (Table 1). In the case of fragments 2, it was twice as high, and even higher for fragments 1.

Mobility of ATEMPO embedded into membranes has been characterized by effective rotational correlation time (τ_{eff}) of the spin probe, which was calculated from EPR spectra (Fig. 4) according to the following formula [19]:

$$\tau_{eff} = 6.6 \cdot 10^{-10} \Delta H_{+1} [(I_{+1}/I_{-1})^{1/2} - 1],$$

Fig. 2. EPR spectra of ATEMPO in chloroplasts (a), subchloroplast fragments 1 (b), subchloroplast fragments 2 (c), and supernatant above chloroplast pellet (d) at 25°C. Samples for EPR measurements were obtained after incubation of chloroplasts or subchloroplast fragments with ATEMPO, centrifugation, and resuspending of the pellet in Tricine buffer (pH 7.5).

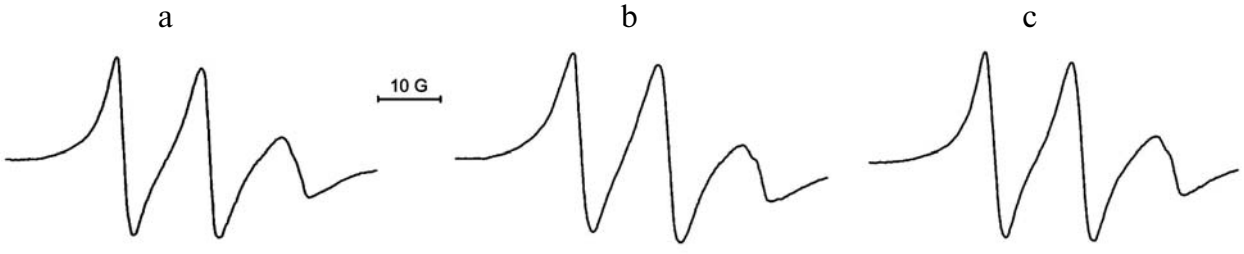

Fig. 3. EPR spectra of ATEMPO incorporated into chloroplasts (a), subchloroplast fragments 1 (b), and subchloroplast fragments 2 (c). EPR spectra were obtained after incubation of chloroplasts or subchloroplast fragments with ATEMPO and double centrifugation. The pellets were suspended in Tricine buffer, pH 7.5. EPR spectra were registered at 25°C.

Table 1. Partitioning of ATEMPO (p) between the aqueous phase and the membrane structures and τ_{eff} of ATEMPO in the membranes of chloroplasts and subchloroplast fragments (25°C)

Object	p*	τ_{eff}, nsec
Chloroplasts	0.07	1.49
Fragments 1	0.21	1.93
Fragments 2	0.15	1.71

* Calculated as a ratio of the intensities of narrow and wide high-field line components in EPR spectra.

where ΔH_{+1} is line-width of the EPR low-field hyperfine line and I_{+1} and I_{-1} are the heights of the low- and high-field lines, respectively.

The estimated values of τ_{eff} for chloroplasts and the fragments at 25°C ranged approximately from 1.5 to 1.9 nsec (Table 1) and are related to the border of fast-motional and slow-motional regimes. Figure 4 demonstrates EPR spectra of immobilized ATEMPO measured at various temperatures in the range 25-60°C. The analysis of the effective correlation times calculated from these spectra showed that τ_{eff} decreases with increasing temperature in the range 25-40°C (Fig. 5a). The lowest values of τ_{eff} are observed for chloroplasts in the whole temperature range. τ_{eff} values of our spin probe located in fragments 2 are higher than those for chloroplasts. The highest τ_{eff} values are observed for fragments 1. In the case of fragments 1 and 2, τ_{eff} values do not significantly differ at the temperatures above 40°C.

The analysis of a temperature dependence of τ_{eff} expressed in Arrhenius coordinates as $\{\ln(1/\tau_{eff} \cdot T) - 1/T\}$ displays different slope for fragments 1 in comparison with those for chloroplasts and fragments 2 (Fig. 5b). Within the temperature range used in this investigation, the slopes of linear Arrhenius plots for the latter are more similar. These data suggest different surrounding of the spin probe localized in the membranes of chloroplasts and fragments 1 and 2. On the basis of the equation

$$1/(\tau_{eff} \cdot T) = (k/h)\cdot\exp(\Delta S^{\#}/R)\cdot\exp(-\Delta H^{\#}/RT),$$

the apparent activation enthalpy ($\Delta H^{\#}$) and entropy ($\Delta S^{\#}$) of ATEMPO rotational motion were calculated as well as an apparent free energy of activation ($\Delta G^{\#}$) (Table 2).

The binding of ATEMPO by chloroplasts and subchloroplast fragments was found to induce changes in photooxidation of P700. Figure 6 shows changes in kinetics of P700 oxidation and dark recovering evoked by the radical binding by chloroplasts. When the actinic light is turned on, the P700 is oxidized which is accompanied by the absorbance decrease, so-called bleaching. Significant decrease in the maximal level of P700 signal (maximal bleaching), 5.3 times, is displayed. The time of reaching this level, as well as the relaxation time to the dark level is less for the sample to which ATEMPO has been added:

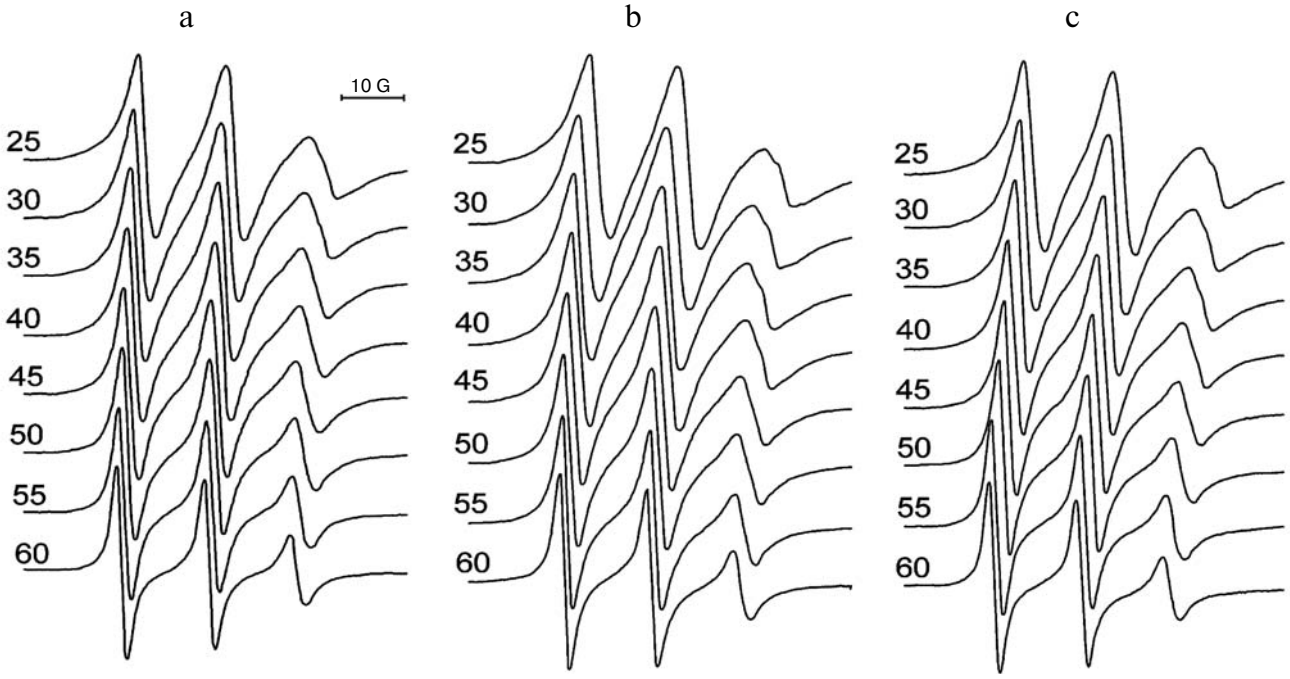

Fig. 4. EPR spectra of ATEMPO incorporated into chloroplasts and subchloroplast fragments 1 and 2 (a, b, and c, respectively). The spectra were recorded at various temperatures from 25 to 60°C (numbers by the curves).

Table 2. Apparent activation parameters of ATEMPO rotational motion in membranes of chloroplasts and subchloroplast fragments

Object	$\Delta H^{\#}$, kJ/mol	$\Delta S^{\#}$, entropy units	$\Delta G^{\#}$, kJ/mol*
Chloroplasts	11.74 ± 0.53	−8.72 ± 0.09	22.61
Fragments 1	15.18 ± 0.44	−5.89 ± 0.05	23.23
Fragments 2	13.18 ± 0.43	−7.82 ± 0.06	22.92

* Calculated from $\Delta G^{\#} = \Delta H^{\#} - T\Delta S^{\#}$ for temperature 298 K.

2.6 times for time of rise and 1.8 times for dark relaxation. The shape of the kinetic curves after achievement of a maximum and before turning off the actinic light is also different. These data coincide for samples washed and not washed free from excess amount of the probe. Similar changes were also revealed for subchloroplast fragments.

DISCUSSION

Analyzing the two-component EPR spectrum of nitroxyl radical which is present in pellets of chloroplasts and the subchloroplast fragments, we conclude that ATEMPO binds to the membrane structures of these particles. Two components due to superposition of EPR signals correspond to various microenvironment of the spin probe. The wide components correspond to the bound state of ATEMPO in a membrane because they remain in the spectrum after washing of pellets of chloroplasts and the subchloroplast fragments. The narrow components, which disappeared after washing, obviously caused by presence of unbound radical fraction in a residual amount of buffer in the pellets, or a radical fraction slightly sorbed on the surface of the bioparticles in a hydrophilic surrounding. The result of the washing is practically identical in all the investigated samples, and it suggests that the first assumption is more plausible.

The EPR spectra of ATEMPO presented in Fig. 2 (a-c) demonstrate the difference in ratio of the narrow and wide components in the high-field lines for chloroplasts and fragments 1 and 2. Computing the ratio of their intensities shows the same (Table 1). Since only wet pellets without the residual supernatant above them were used, then the amount of the free ATEMPO fraction has to be the same in all types of pellets. Therefore, the ratio of intensities of the narrow and wide components can be an estimation of a share of membrane-bound ATEMPO fraction. Table 1 demonstrates that this share is the smallest for chloroplasts and the greatest for fragments 1. The distinction between chloroplasts and the fragments can be explained by difference in the number of ATEMPO binding sites in these objects. For example, chloroplasts contain intergranal thylakoids, which are absent in our subchloroplast fragments. Fragments 1 and 2 can differ from each other and from chloroplasts both by number of sites of binding, and by possibility for the probe to permeate into the corresponding sites. Granal structures in fragments 2 are more damaged and therefore penetration of our probe into them can be easier.

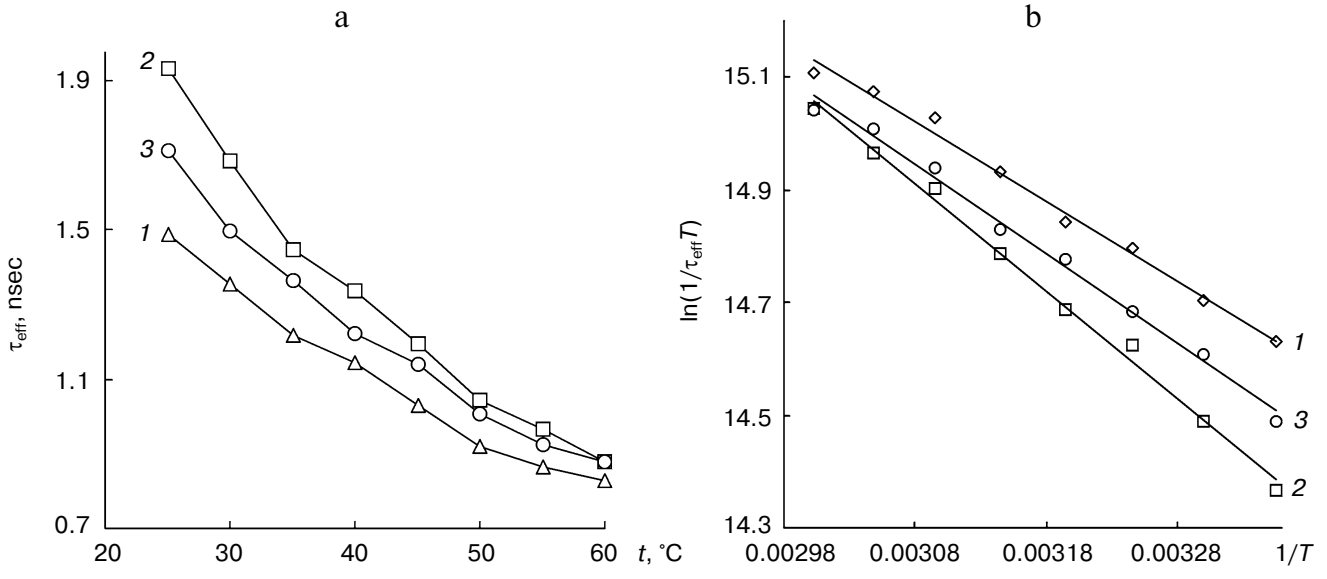

Fig. 5. a) Temperature dependences of the effective rotational correlation time (τ_{eff}) derived from EPR spectra of ATEMPO incorporated into chloroplasts (*1*), subchloroplast fragments 1 (*2*), and subchloroplast fragments 2 (*3*). b) Linear anamorphosis of temperature dependences of τ_{eff} ATEMPO incorporated into chloroplasts (*1*), subchloroplast fragments 1 (*2*), and subchloroplast fragments 2 (*3*).

The spin labeled compound ATEMPO residing completely in the membrane structures exhibits a different mobility. The effective rotational correlation times τ_{eff} (Table 1) as well as their temperature dependences (Fig. 5) appeared to be different for chloroplasts and their fragments. It should be noted that the smallest τ_{eff} is inherent in chloroplasts. It is greater for fragments 2 and even greater for fragments 1. These distinctions in mobility of the probe show differences in the specificity of binding sites in the investigated objects. This conclusion is also confirmed by differences in the activation parameters $\Delta H^{\#}$ and $\Delta S^{\#}$ of rotational motion of ATEMPO bound with chloroplasts and the subchloroplast fragments. The apparent activation enthalpy is the smallest for chloroplasts, higher for fragments 2, and the highest for fragments 1 (Table 2). Thus, these data also reveal difference in the nature of binding sites of ATEMPO in membranes of chloroplasts and the subchloroplast particles. It should be emphasized that calculated τ_{eff} are the average values, the contribution to which gives all possible binding sites of our probe, in each of the investigated objects. As follows from τ_{eff} values (Table 1), chloroplasts contain the largest number of binding sites causing higher mobility of the probe. In contrast, fragments 1 contain the largest quantity of binding sites supplying low mobility.

Binding of ATEMPO by chloroplasts and fragments 1 and 2 causes significant reduction in P700 signal and change of its kinetics (Fig. 6). This suggests that one of the sites of embedding of our spin probe can be the nearest surrounding of PSI pigment–protein complexes. Possibly, it is a lipid fraction of the complex. It is known that lipids are bound with proteins and the membrane supramolecular complexes. In particular, it was shown that more than 40% of lipid fraction is localized on a surface of proteins in granal membranes [13, 20]. The noncovalent interaction initiates less mobile lipid layers in the nearest surrounding of protein macrocomplexes [12]. The chemical structure of water-insoluble ATEMPO and the effective rotational correlation time which relates to the values on the border between fast- and slow-motional regimes, suggest a mode of its arrangement in the membranes. Obviously, its hydrocarbon fragment is buried into nonpolar sites of lipid domains, while the nitroxyl part is positioned in a polar head group region. Thus, the lipid surrounding of PSI complexes can be a site of binding of ATEMPO.

Removing of the intergranal thylakoids, which, as it is known, are abundant with PSI complexes, results in a decrease in a share of bound probe as follows from comparison of EPR spectra of chloroplasts and fragments 1 (Fig. 2). The content of PSI complexes in fragments 1 is lower as has been shown with the low temperature fluorescence spectra [8]. The amount of membrane-associated ATEMPO in fragments 1 is also lower as shown by comparison of the intensity ratios of the narrow and wide components in the high-field EPR lines (Table 1). Thus,

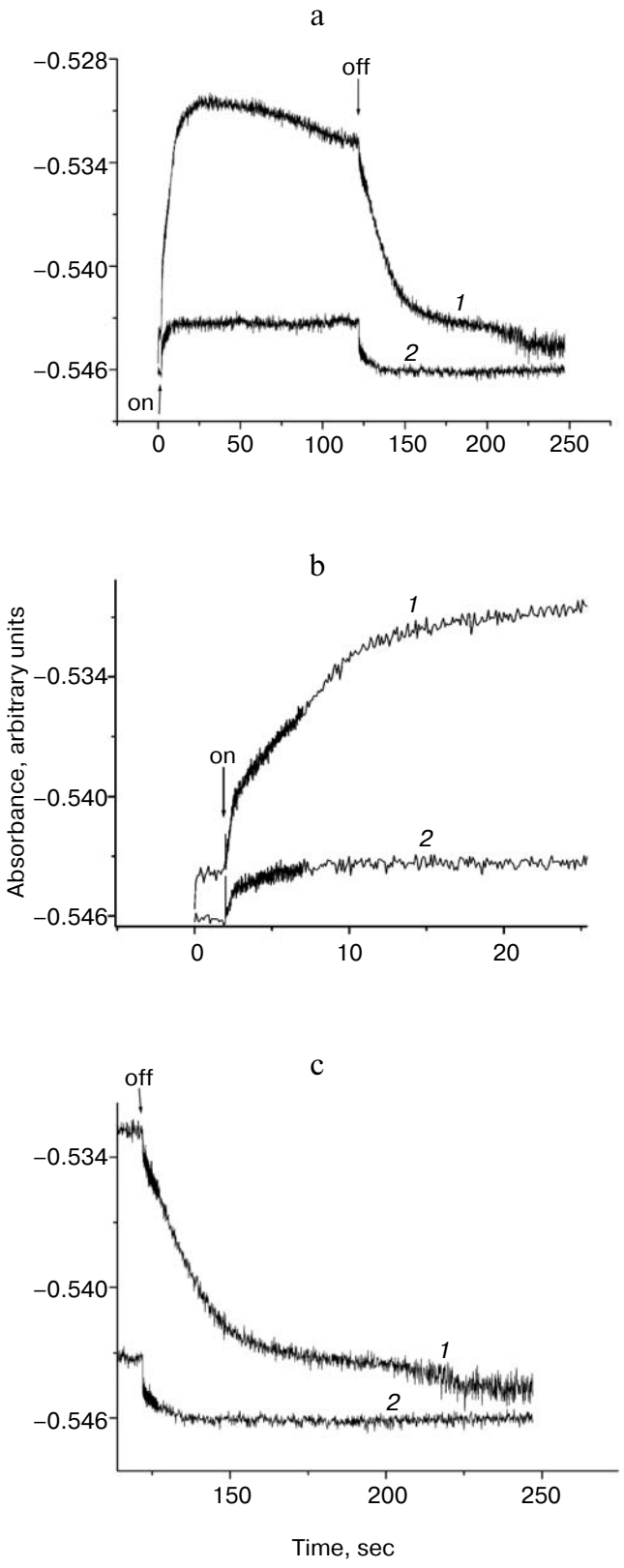

Fig. 6. Kinetics of P700 oxidation and dark reduction in chloroplasts without (*1*) and with ATEMPO addition (*2*) (a); (b) and (c) are the initial and the final parts of P700 kinetics (a).

this observation is in a good accordance with the assumption that the nearest surrounding of PSI complexes is one of the types of the binding sites. In accordance with our data, the share of membrane-bound ATEMPO is greater for fragments 2 than for fragments 1, although the former are depleted of PSI complexes [8]. This must mean that there are the binding sites of other types in fragments 2. They are, obviously, regions of PSII or LHCII (light-harvesting complex of PSII) complexes. Both of them become more open in fragments 2 due to removing of the thylakoid margins.

Comparative analysis of effective rotational correlation times and the temperature dependences of τ_{eff} for spin probe in the studied objects demonstrates the following. The value of τ_{eff} is higher for subchloroplast fragments 1 in comparison with chloroplasts. Note that subchloroplast fragments 1 are abundant predominantly with PSIα complexes but depleted in intergranal thylakoids containing PSIβ complexes. The ratio PSIα/PSIβ is 4 : 1 for chloroplasts according to Albertson's model [21]. Thus, higher relative content of PSIβ in chloroplasts corresponds to lower τ_{eff}, i.e. higher mobility of nitroxyl radical. This fact shows the difference in state of spin probe bound in near surroundings of PSIα and PSIβ. Change in activation parameters of ATEMPO rotational diffusion, such as entropy and enthalpy induced by its binding with chloroplasts and subchloroplast fragments 1 confirms the supposition. It is also in good correspondence with other literature data. They are as follows. PSIα complexes have a greater light-harvesting antenna containing specific proteins that cause its difference from light-harvesting complexes of PSIβ and PSII [7]. Our data concerning excitation spectra of low temperature fluorescence also revealed larger size of PSIα light-harvesting antenna in comparison with the one in PSIβ as well as differences in the set of spectral forms of chlorophylls [4, 6, 9, 10]. The presence of specific lipids on marginal regions of granal thylakoids [20] can indicate peculiarities in organization of lipid surrounding PSIα complexes located in this region of granal thylakoids.

It is important to note that τ_{eff} in subchloroplast fragments 2 (which contain only low amount of PSIα complex, while PSIβ complexes are almost absent in them) was lower in comparison with fragments 1 but higher in comparison with chloroplasts. This may be caused by possible binding of spin probe also with PSII complexes and/or with LHCII. This possibility needs further studies.

REFERENCES

1. Albertsson, P.-A. (1995) *Photosynth. Res.*, **46**, 141-149.
2. Andersson, B., and Anderson, J. M. (1980) *Biochim. Biophys. Acta*, **593**, 427-440.
3. Anderson, J. M. (1989) *Physiol. Plant.*, **76**, 243-248.
4. Kochubey, S. M. (2001) *Russ. J. Plant Physiol.*, **48**, 333-339.
5. Gadjieva, R., Mamedov, F., and Albertsson, P.-A. (1999) *Biochim. Biophys. Acta*, **1411**, 92-100.
6. Kochubey, S. M., Shevchenko, V. V., and Bondarenko, O. Yu. (2004) *Russ. J. Plant Physiol.*, **51**, 147-151.
7. Andreasson, E., and Albertsson, P.-A. (1993) *Biochim. Biophys. Acta*, **1141**, 175-182.
8. Kochubey, S. M., Shevchenko, V. V., and Bondarenko, O. Yu. (2005) *Dokl. NAN Ukrainy*, **4**, 161-166.
9. Kochubey, S. M. (2001) *Organization of Photosynthetic Apparatus of Higher Plants* (Morgoun, V. V., ed.), Alterpress, Kiev.
10. Kochubei, S. M., Shevchenko, V. V., and Bondarenko, O. Yu. (2003) *Russ. J. Plant Physiol.*, **50**, 287-292.
11. Li, G., Knowles, P. F., Murphy, D. J., and Marsh, D. (1990) *J. Biol. Chem.*, **265**, 16867-16872.
12. Li, G., Knowles, P. F., Murphy, D. J., Nishida, I., and Marsh, D. (1989) *Biochemistry*, **28**, 7446-7452.
13. Pali, T., Garab, G., Horvath, L. I., and Kota, Z. (2003) *Cell. Mol. Life Sci.*, **60**, 1591-1606.
14. Kota, Z., Horvath, L. I., Droppa, M., Horvath, G., Farkas, T., and Pali, T. (2002) *Proc. Natl. Acad. Sci. USA*, **99**, 12149-12154.
15. Wasniowska, A., Subczynski, W. K., and Tikhonov, A. (2002) *Curr. Top. Biophys.*, **26**, 83-91.
16. Vovk, A. I., Kharchenko, O. V., Kharitonenko, A. I., Kukhar, V. P., Babii, L. V., Kazachkov, M. G., Melnyk, A. K., and Khilchevsky, A. N. (2004) *Russ. J. Bioorg. Chem.*, **30**, 391-395.
17. Kochubey, S. M., Volovik, O. I., Korneev, D. Yu., Porubleva, L. V., and Shevchenko, V. V. (1998) *Russ. J. Plant Physiol.*, **45**, 695-701.
18. Muehlenbein, H., and Schlirkamp-Voosen, D. (1993) *Evolut. Comput.*, **1**, 25-49.
19. Buchachenko, A. L., and Wasserman, A. M. (1973) *Stable Radicals* [in Russian], Khimiya, Moscow.
20. Garab, G., Lohner, K., Laggner, P., and Farkas, T. (2000) *Trends Plant Sci.*, **5**, 489-494.
21. Albertsson, P.-A. (2001) *Trends Plant Sci.*, **6**, 349-354.